SUPPLEMENTARY INFORMATION

FOR

Tetradecanuclear Iron(III)-Oxo Nanoclusters Stabilized by Trilacunary Heteropolyanions

Masooma Ibrahim,[†,▽] Ali Haider,[†] Yixian Xiang,[†] Bassem S. Bassil,[†,‡] Akina M. Carey,[†] Lisa Rullik,[†] Geoffrey B. Jameson,[#] Floriant Doungmene,[§] Israël M. Mbomekallé,*[,§] Pedro de Oliveira,[§] Valeriu Mereacre,[∥] George E. Kostakis,[▵] Annie K. Powell,*[,∥,⊥] and Ulrich Kortz*[,†]

[†]Department of Life Sciences and Chemistry, Jacobs University, P.O. Box 750 561, 28725 Bremen, Germany

[‡]Department of Chemistry, Faculty of Sciences, University of Balamand, P.O. Box 100, Tripoli, Lebanon

#Institute of Fundamental Sciences, Massey University, Tennent Drive, Palmerston North 4442, New Zealand

[§]Equipe d'Electrochimie et de Photoélectrochimie, Laboratoire de Chimie-Physique, Université Paris-Sud, UMR 8000 CNRS, Orsay F-91405, France

[∥]Institute of Inorganic Chemistry, Karlsruhe Institute of Technology (KIT), Engesserstrasse 15, 76131 Karlsruhe, Germany

[▵]Department of Chemistry, School of Life Sciences, University of Sussex, Brighton BN1 9QJ, United Kingdom

[⊥]Institute of Nanotechnology, Karlsruhe Institute of Technology (KIT), Hermann-von-Helmholtz Platz 1, 76344 Eggenstein-Leopoldshafen, Germany

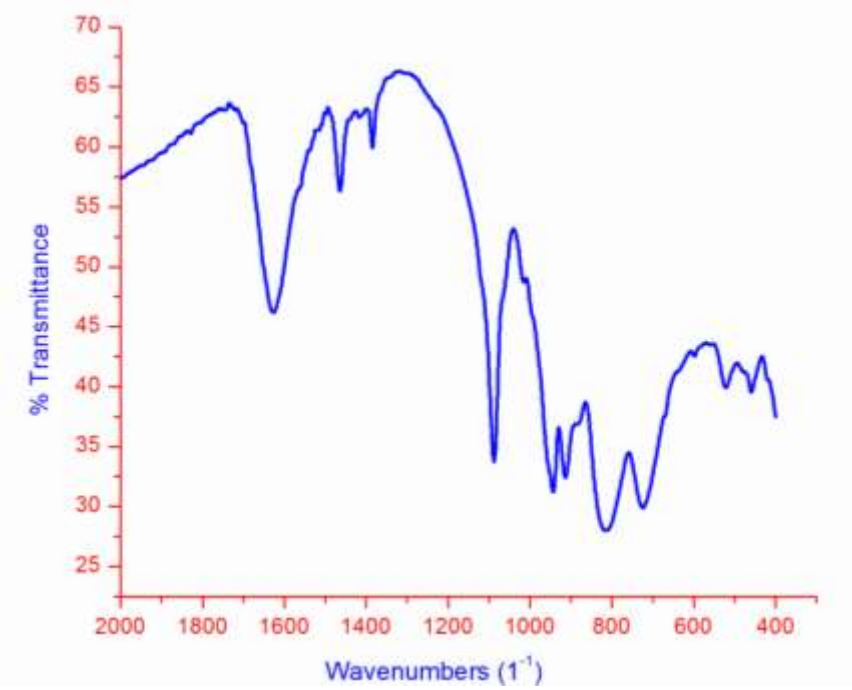

Figure S1. IR spectrum of **GuNa-1**.

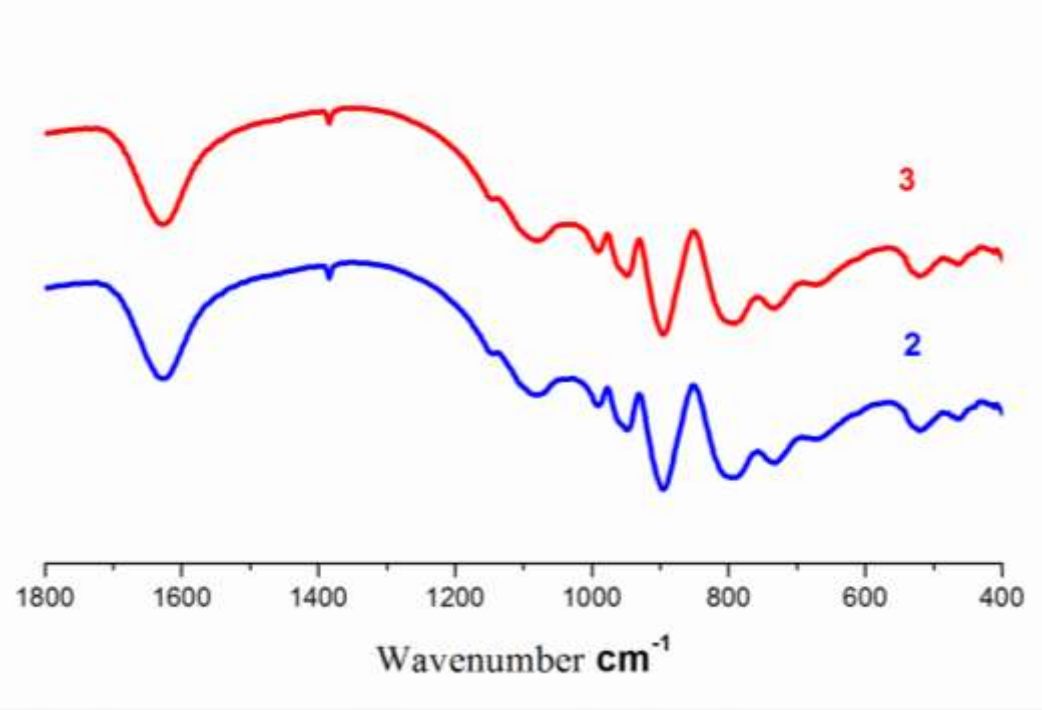

Figure S2. IR spectra of **CsKNa-2** and **RbNa-3**.

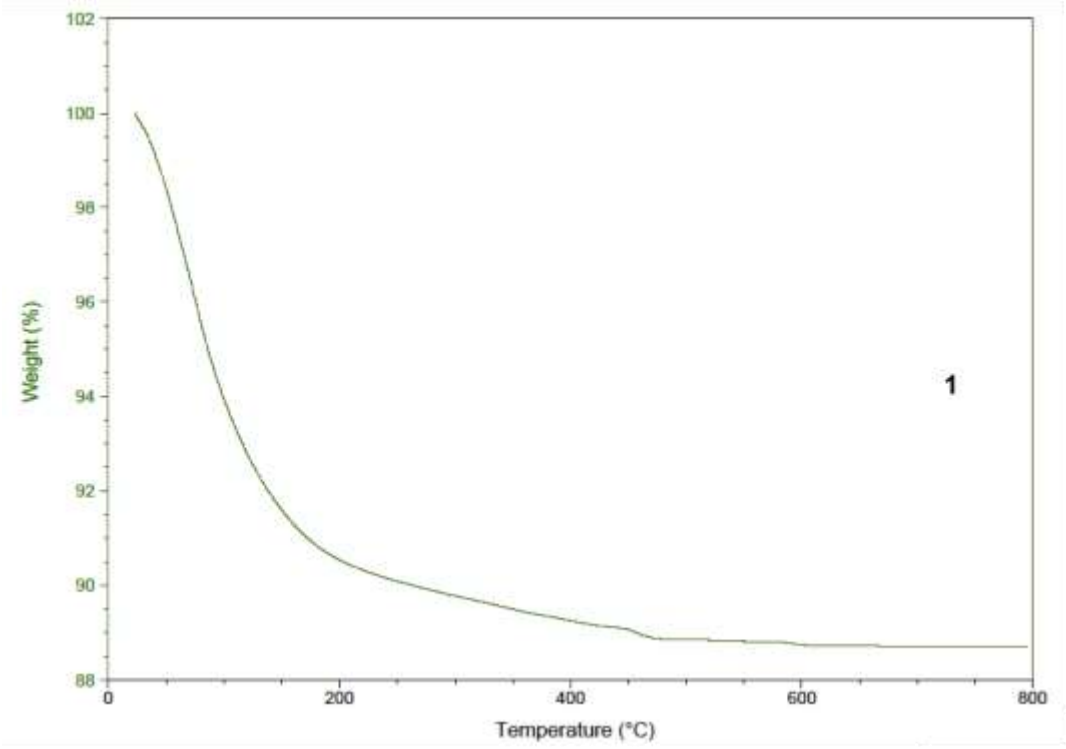

Figure S3. Thermogram of **GuNa-1**.

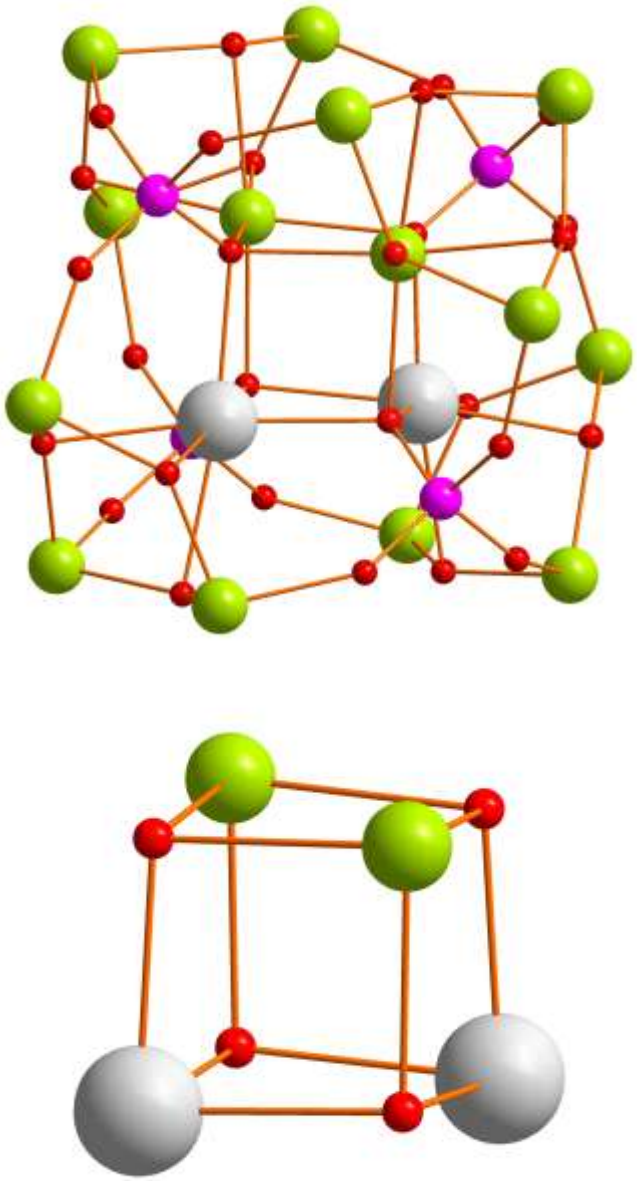

Figure S4. Top: Ball-and-stick representation of $[Na_2Fe^{III}_{14}(OH)_{12}(PO_4)_4]^{20-}$, bottom: representation of the $\{Na_2Fe_2O_4\}$ cubane core. Color code: Fe (lime), oxygen (red), sodium (light-grey).

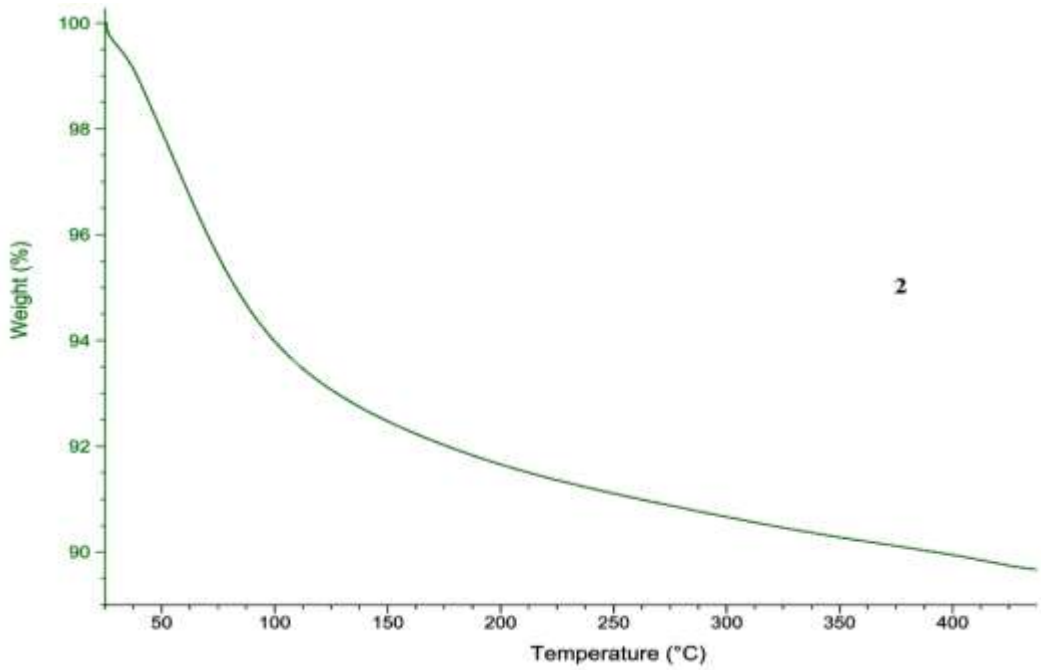

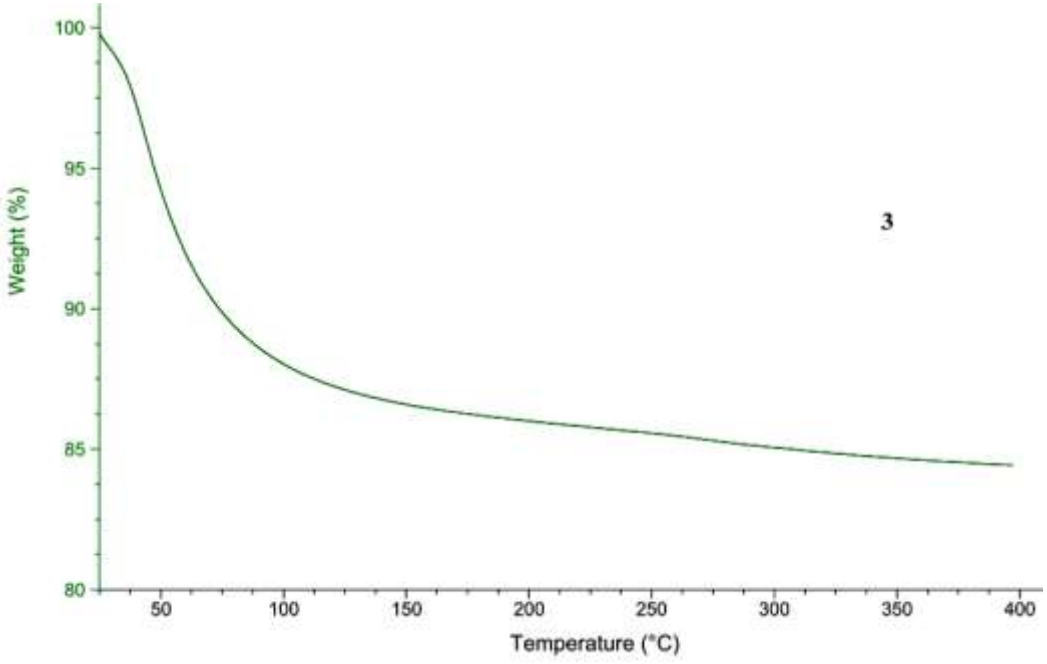

Figure S5. Thermogram of **CsKNa-2** (top) and **RbNa-3** (bottom).

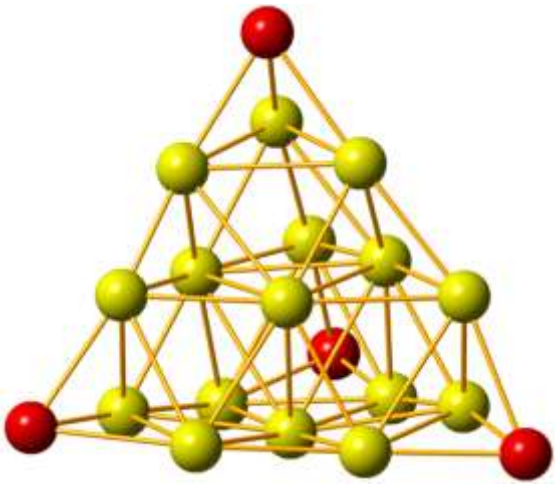

Figure S6. The super-tetrahedron (*T*3) motif found in Mn_{20}, highlighting the four missing corners, to show the structural similarity with the Fe_{16} core.

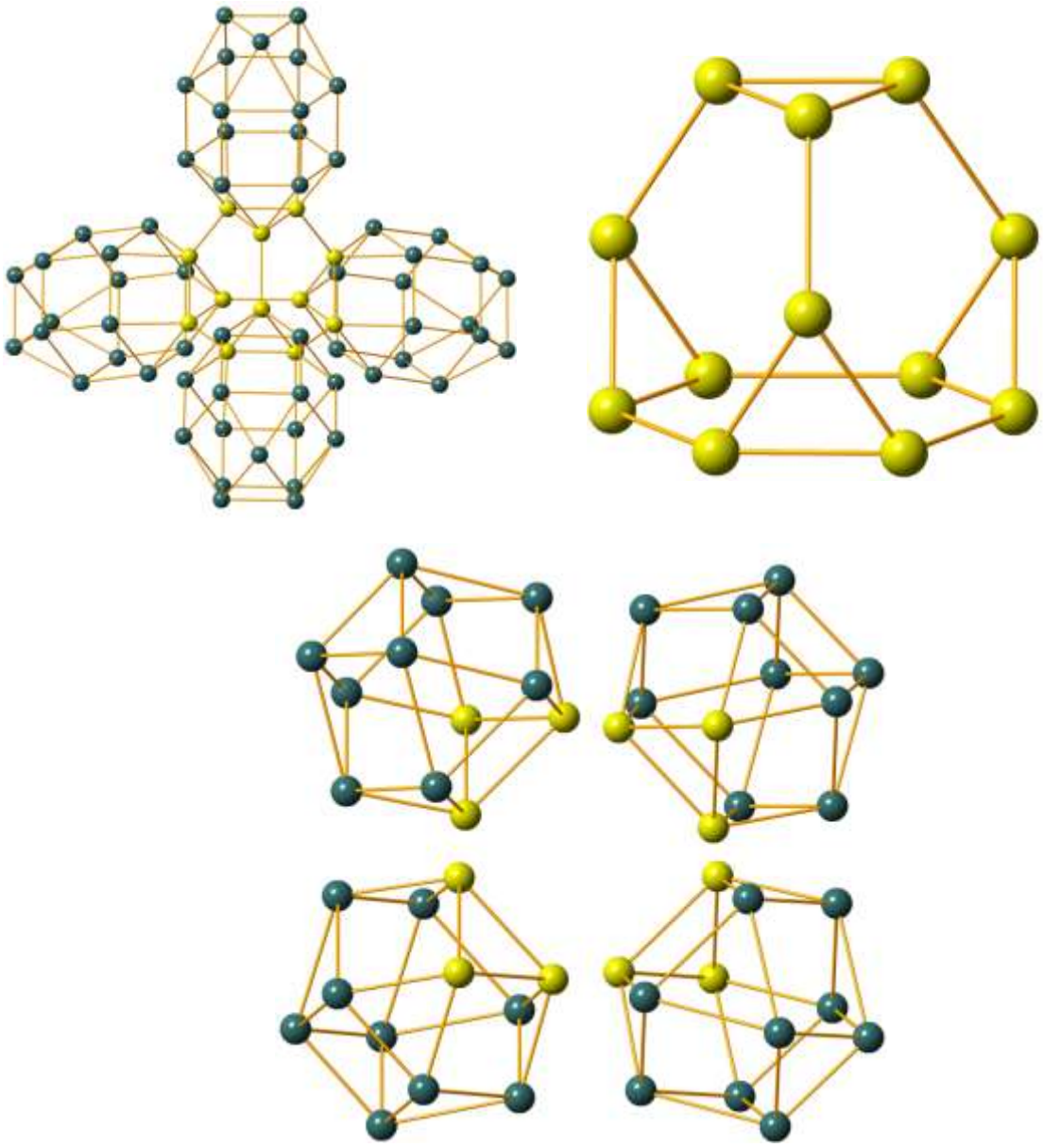

Figure S7. (Upper) The decorated motifs for polyanion **1**, **4,4,4,5M72-1** (left), and **3M12-1** (right) excluding the inner four Fe ions from the simplification process. (Lower) The decorated motif for polyanions **2** and **3**, **4(4M12-1)** excluding the inner four Fe ions from the simplification process.

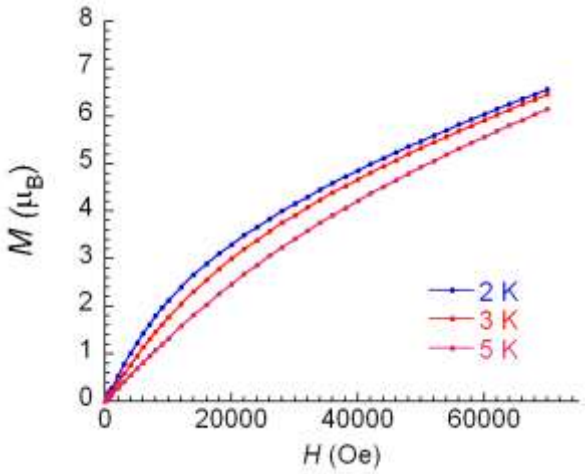

Figure S8. Field dependence of magnetization at low temperatures for **GuNa-1**.

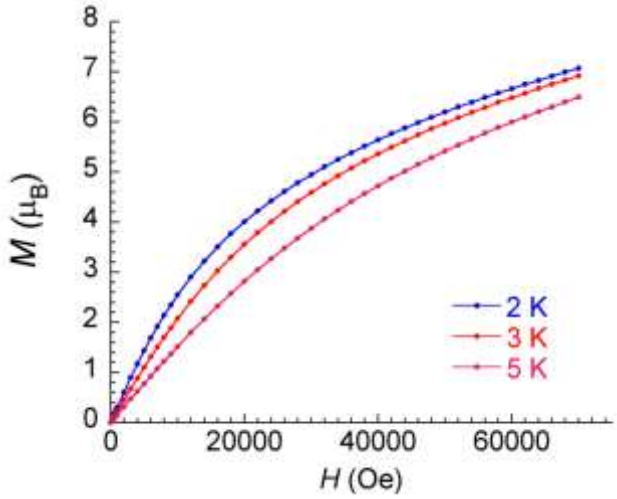

Figure S9. Field dependence of magnetization at low temperatures for **CsKNa-2**.

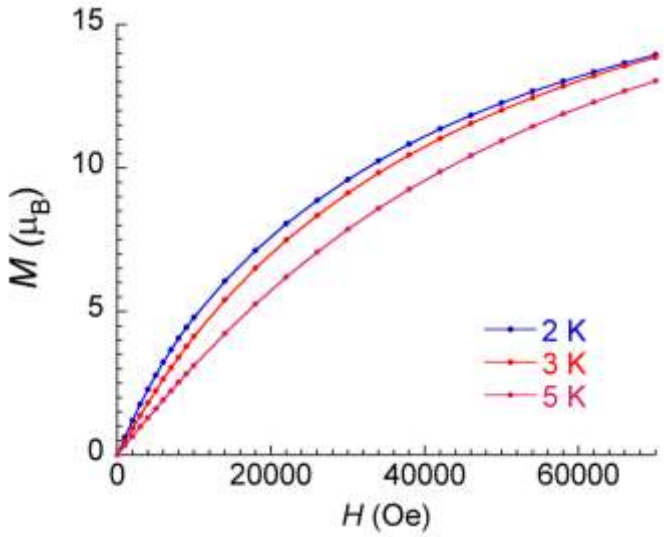

Figure S10. Field dependence of magnetization at low temperatures for **RbNa-3**.

1. Electrolysis of 1 in 1.0 M $LiCH_3COO + CH_3COOH$ / pH 5.

The electrolysis potential was set at -0.48 V vs. SCE. The total charge passed during the process was 563 mC for 4.0×10^{-4} mmol of **1**, which is 14.5 moles of electrons per mole of **1**. During the electrolysis, the solution colour changed from yellow to pale green. The blue colour indicative of the reduction of W^{VI} centres was not observed, proving that just the Fe^{3+} centers were reduced in this case.

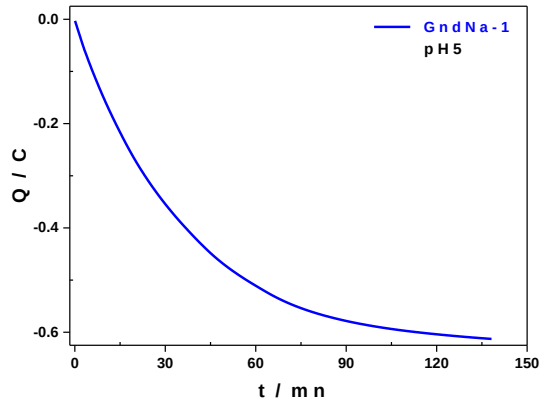

Figure S11. Charge passed as a function of time. Working electrode: glassy carbon plate; counter electrode: platinum gauze placed in a compartment separated from the main solution by a fritted glass; reference electrode: SCE placed in a compartment separated from the main solution by a fritted glass.

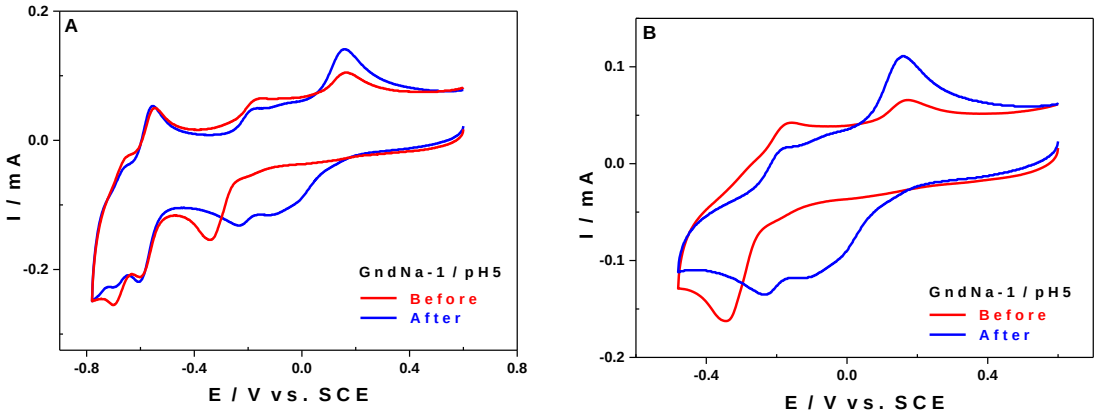

Figure S12. Evolution of the cyclic voltammograms of **1** before electrolysis (consisting of a total reduction of the Fe^{3+} centers at -0.48 V vs. SCE (red)) and after total re-oxidation of all the Fe^{2+} centers generated by the previous reaction (blue). (A) The voltammograms include the first waves involving the W centres; (B) Voltammograms restricted to the waves concerning the Fe centers.

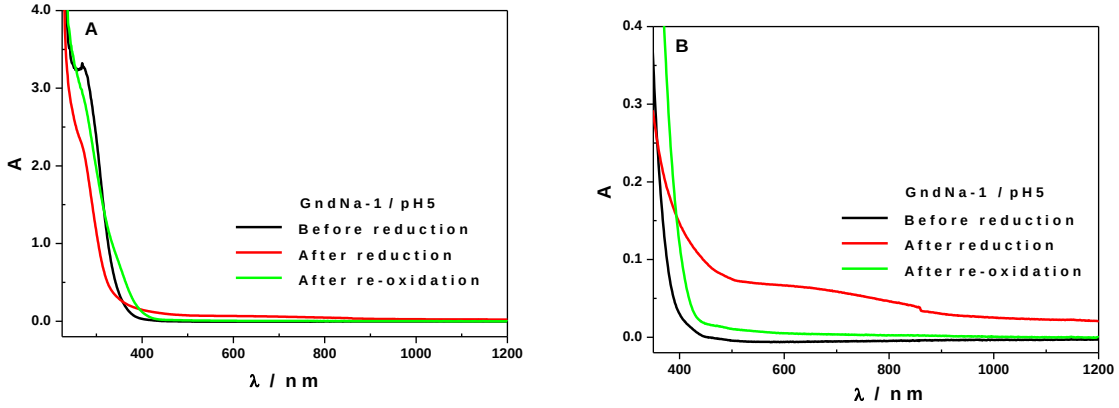

Figure S13. Evolution of the UV-visible spectra of a solution of **1** (0.08 mM) before reduction (black), after reduction (red) and after re-oxidation (green).

2. Electrochemical behaviour of GndNa-1 in 1.0 M $LiCH_3COO + CH_3COOH$ / pH 6.

Figure S14-A shows two successive CVs of **1** in 1.0 M $LiCH_3COO + CH_3COOH$ / pH 6. The black curve corresponds to the first CV obtained with a freshly polished electrode. The same waves as in a pH 5 medium are observed (see main text and Figure 9). The red curve corresponds to the second CV and was registered right after the first one. There is a new reduction wave, which is more positive than the others and peaks at -0.13 V vs. SCE. We have suggested that this wave is due to the reduction of non-coordinated Fe^{3+} which is detached from **1** upon reduction. In order to confirm this hypothesis, the potential range has been restricted to the Fe^{3+} centers reduction waves, therefore excluding the waves attributed to the W^{VI} centers ($E_{reverse}$ = -0.60 V vs. SCE, Figure S14-B). It is clear that the formation of the mentioned new wave is due to the Fe^{3+} centers which are removed from **1** upon reduction to Fe^{2+}. Bearing in mind that the pH of the solution is 6, it is highly likely that the re-oxidised, free Fe^{3+} ions give rise to hydroxides and oxides which adsorb to the working electrode surface. These insoluble

hydroxides and oxides are, then, the first to be reduced upon a second reduction cycle, resulting in the formation of a new, more positive reduction wave at -0.13 V vs. SCE. The wave observed in the first CV has lost in intensity but remains at the same potential of -0.41 V vs. SCE. When successive cycling is performed on the new wave ($E_{reverse}$ = -0.18 V vs. SCE, Figure S14-C), it quickly disappears, a common method to regenerate the working electrode surface.

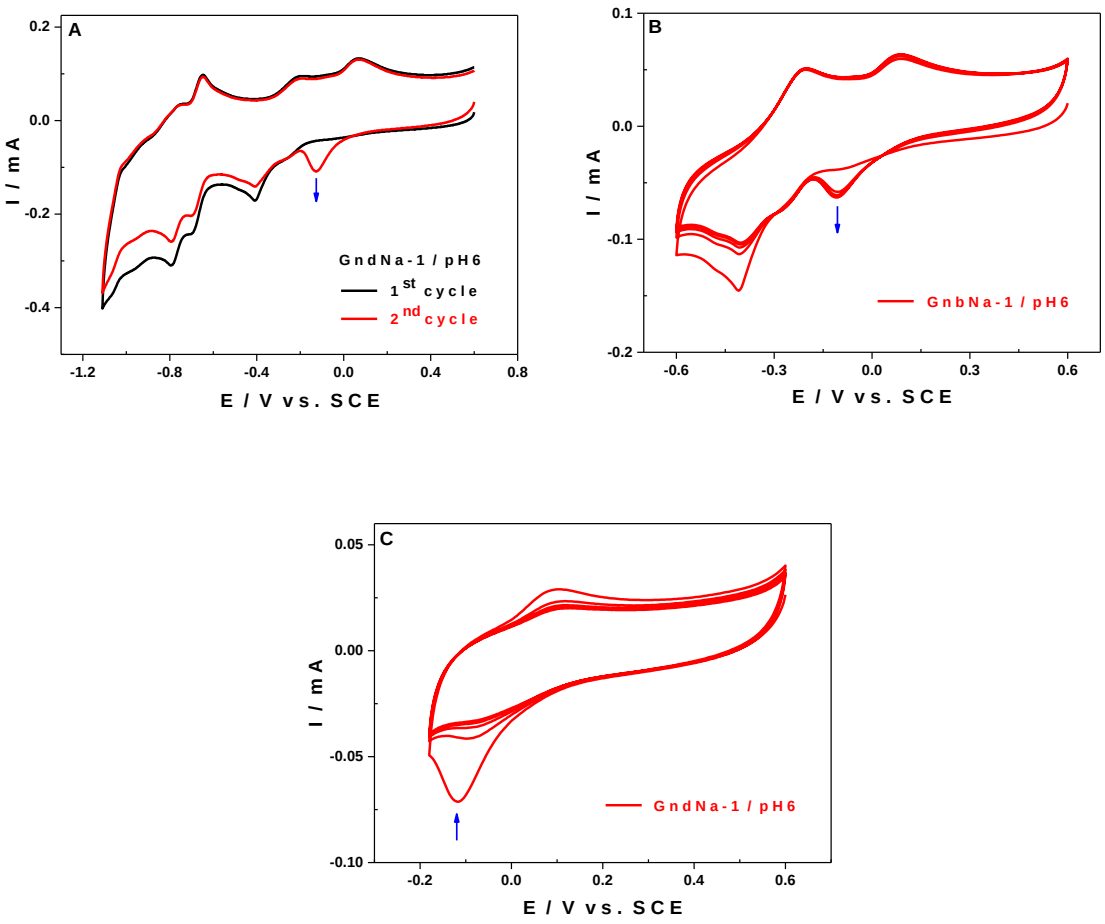

Figure S14. Cyclic voltammograms of **1** in 1.0 M $LiCH_3COO$ + CH_3COOH / pH 6. Scan rate: 10 mV s^{-1}; working electrode: glassy carbon; reference electrode: SCE. (A) 1^{st} cycle (black) and 2^{nd} cycle (red) extended up to the W center waves, $E_{reverse}$ = -0.89 V vs. SCE. (B) Cyclic voltammograms restricted to the Fe center waves, 5 consecutive cycles, $E_{reverse}$ = -0.60 V vs. SCE. (C) Cyclic voltammograms restricted to the new wave corresponding to electro-deposited Fe hydroxides, $E_{reverse}$ = -0.18 V vs. SCE.

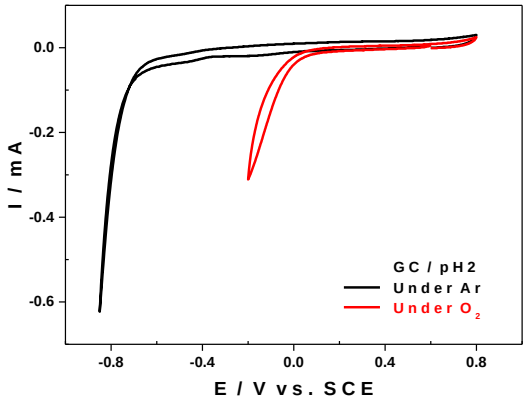

Figure S15. Cyclic voltammograms obtained with a glassy carbon working electrode in 0.5 M Li_2SO_4 + H_2SO_4 / pH 2, under argon (black) and under di-oxygen (red). Scan rate: 2 $mV.s^{-1}$; reference electrode: SCE.

3. Electrochemical behaviour of 2 and 3 in 0.5 M Li_2SO_4 + H_2SO_4 / pH 3 and in 1.0 M $LiCH_3COO$ + CH_3COOH / pH 5.

Unlike polyanion **1**, which is stable in media having pH values comprised between 2 and 6, polyanions **2** and **3** are not stable in several aqueous buffers tested. In sulfate medium (0.5 M Li_2SO_4 + H_2SO_4 / pH 3) they slowly decay with a concomitant loss of Fe^{3+} ions. On the other hand, they exhibit a higher stability in acetate medium (1.0 M $LiCH_3COO$ + CH_3COOH / pH 5). Despite this drawback, we were able to characterise them by cyclic voltammetry upon recording the CVs just after dissolution. As expected, polyanion **2**, which contains $\{SiW_9\}$ fragments, is more difficult to reduce than polyanion **3**, which is based on $\{GeW_9\}$ fragments, in agreement

with the conclusions drawn from our previous study concerning the dependence of Keggin-type POM redox potentials on the nature of the hetero-atom X (X = B, Al, Ga, Si, Ge, P and As).[1]

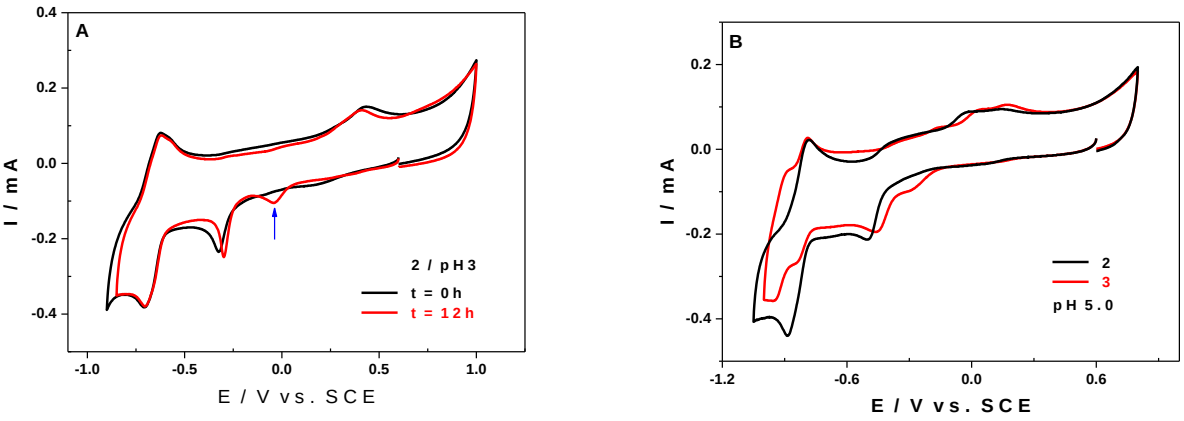

Figure S16. (A) CVs of **2** in 0.5 M Li_2SO_4 + H_2SO_4 / pH 3.0. The first CV was recorded right after the solubilisation of the compound, at t = 0 (black), and another one after 12 h (red). (B) CVs of **2** (black) and **3** (red) in 1.0 M $LiCH_3COO$ + CH_3COOH / pH 5.0. POM concentration: 0.08 mM; working electrode: glassy carbon; counter electrode: Pt; reference electrode: SCE; scan rate: 10 mV s^{-1}.

Controlled potential coulometry experiments were carried out at pH 5 (1.0 M $LiCH_3COO$ + CH_3COOH) with the potential set at -0.70 V vs. SCE for polyanions **2** and **3**, i.e. a sufficiently negative value in order to reduce all the Fe^{3+} centers in the polyanion without interfering with the W^{VI} centers, which are reduced at more negative potentials. The total charge that crosses the system during the experiments was 502 mC and 515 mC for 4.3×10^{-4} mmol of **2** and 4.0×10^{-4} mmol of **3** in solution, respectively. This corresponds to the reduction of almost all the Fe^{3+} centers present in each compound (12 for **2** and 13.5 for **3**). Similarly to polyanion **1**, this

operation leads to a structural rearrangement of the two polyanions as well, which results in the CVs recorded after total re-oxidation (E = +0.70 V vs. SCE) being different from the ones at the beginning. The waves corresponding to the reduction of the Fe^{3+} centers are shifted towards more positive potentials and are split, whereas those attributed to the reduction of the W^{VI} centres keep the same shapes and positions.

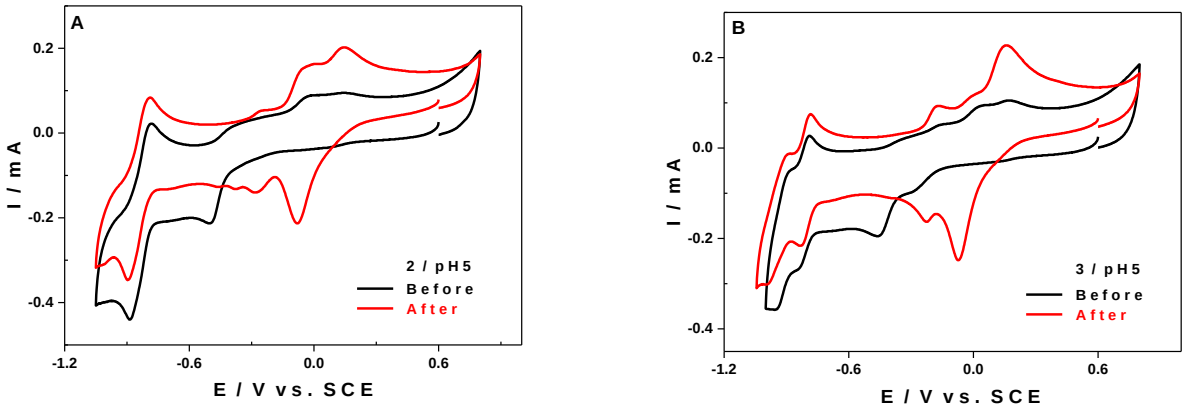

Figure S17. (A) CVs of **2** and (B) CVs of **3** in 1.0 M $LiCH_3COO$ + CH_3COOH / pH 5.0, before reduction at -0.7 V vs. SCE (black) and after re-oxidation at +0.7 V vs. SCE (red). POM concentration: 0.08 mM; working electrode: glassy carbon; counter electrode: Pt; reference electrode: SCE; scan rate: 10 mV s^{-1}.

References

1. Mbomekallé, I. M.; López, X.; Poblet, J. M.; Sécheresse, F.; Keita, B.; Nadjo, L. *Inorg. Chem.* **2010**, 49, 7001–7006.

Table S1. Selected bond valence sum (BVS) values for $[Fe_{14}(OH)_{13}O_6\{\alpha\text{-}P_2W_{15}O_{56}\}_4]^{31-}$ (**1**).

μ_3-O	BVS Value	Fe Center	BVS Value
O35F	1.450	Fe3	3.068
O36 F	1.105	Fe4	3.021
O24F	1.126	Fe5	3.098
O14	1.153	Fe6	3.272
O15F	1.015		
O12F	1.030		
μ_3-O	BVS Value		
O14	1.826		
O36F	1.862		
O15F	1.824		
μ_3-O	BVS Value		
O2PA	1.858		
O2P2	1.844		

Table S2. Selected bond valence sum (BVS) values for $[Fe^{III}_{14}(OH)_{12}(PO_4)_4(A\text{-}\alpha\text{-}SiW_9O_{34})_4]^{22-}$ (**2**).

μ_3-O (3Fe-O)	**BVS Value**	**Fe**	**BVS value**
O123	1.25	Fe1	3.13
O12F	1.31	Fe3	2.92
O456	1.32	Fe4	3.05
O45F	1.23	Fe5	2.94
μ_2-O (Fe-O-P)		**P**	
O3P1	2.01	P1	5.20
O1P2	1.73	P2	4.89
O3P2	1.84		
O2P1	2.04		
μ_4-O (3Fe-O-P)			
O1P1	1.71		
O2P2	1.94		

Table S3. Selected bond valence sum (BVS) values for $[Fe^{III}_{14}(OH)_{12}(PO_4)_4(A\text{-}\alpha\text{-}GeW_9O_{34})_4]^{22-}$ (**3**).

μ_3-O (Fe-O)	**BVS Value**	**Fe**	**BVS value**
O45E	1.26	Fe1	3.06
O45F	1.22	Fe2	3.11
O12F	1.24	Fe3	3.02
O26F	1.21	Fe4	3.18
μ_2-O (Fe-O-P)		**P**	
O3P1	1.92	P1	5.10
O1P2	1.89	P2	4.94
O3P2	1.91		
O2P1	1.97		
μ_4-O (3Fe-O-P)			
O1P1	1.58		
O2P2	1.53		